



Trans. Nonferrous Met. Soc. China 32(2022) 2598-2608

Transactions of Nonferrous Metals Society of China

www.tnmsc.cn



Microstructure and mechanical behavior of Ti/Cu/Ti laminated composites produced by corrugated and flat rolling

Zhu-bo LIU^{1,2,3}, Xin-yue WANG¹, Ming-shuo LIU¹, Yuan-ming LIU^{1,2,3}, Jiang-lin LIU^{1,2,3}, A. V. IGNATOV⁴, Tao WANG^{1,2,3}

- 1. College of Mechanical and Vehicle Engineering, Taiyuan University of Technology, Taiyuan 030024, China;
 - 2. Advanced Metal Composites Forming Technology and Equipment Engineering Research Center of Ministry of Education, Taiyuan University of Technology, Taiyuan 030024, China;
 - 3. TYUT-UOW Joint Research Center, Taiyuan University of Technology, Taiyuan 030024, China;
- 4. Department of Mechanical Engineering, Bauman Moscow State Technical University, Moscow 105005, Russia

Received 19 July 2021; accepted 15 February 2022

Abstract: Ti/Cu/Ti laminated composites were fabricated by corrugated rolling (CR) and flat rolling (FR) method. Microstructure and mechanical properties of CR and FR laminated composites were investigated by scanning electron microscopy, numerical simulation methods, peel and tensile examinations. The effect of CR and FR was comparatively analyzed. The results showed that the CR and FR laminated composites exhibited different effective plastic strain distributions of the Ti layer and Cu layer at the interface. The recrystallization texture, prismatic texture and pyramidal texture were developed in the Ti layer by CR, while the R-Goss texture and shear texture were developed in the Cu layer by CR. The typical deformation texture components were developed in the Ti layer and Cu layer of FR laminated composites. The CR laminated composites had higher bond strength, tensile strength and ductility.

Key words: Ti/Cu/Ti laminated composites; corrugated rolling; flat rolling; bond strength; interfacial microstructure; finite element analysis

1 Introduction

Titanium (Ti) anodes based on metallic Ti substrate have been widely applied in electrolysis industry due to their excellent corrosion resistance, good electrocatalysis, high mechanical strength and long service life [1–5]. However, the main disadvantage of Ti as an electrode material is its poor electrical properties. In recent years, titanium/copper (Ti/Cu) laminated composites have been fabricated to improve the electrical properties of the Ti substrate with the help of the excellent electrical conductivity and good mechanical properties of metallic Cu [6–11]. Therefore, the Ti/Cu laminated composites not only have the high strength and

corrosion resistance of Ti, but also exhibit the excellent electrical conductivity of Cu. Compared with the anode plate of pure Ti substrate, these laminated composites can reduce the bath voltage and power loss under the same current density, improve the working efficiency, and reduce the production costs [12,13].

For Ti/Cu laminated composites, many preparation methods were introduced, including diffusion bonding [14], indirect extrusion [15], vacuum hot pressing [16], explosive welding [17,18] and roll bonding [19–21]. Among all the above methods, due to simple operating and continuous production, the roll bonding method is commonly used in the fabrication of Ti/Cu laminated composites. Accumulative roll bonding [20] and

cold rolling and subsequent annealing treatment [21] are usually used to fabricate these laminated composites. In order to achieve the bonding of Ti/Cu laminated composites, annealing treatment must be carried out after rolling or during the rolling process. However, a large number of studies on Ti/Cu composites have shown that different types of intermetallic compounds (CuTi, CuTi₂, CuTi₃, Cu₃Ti₂, Cu₄Ti, etc.) can be obtained at different treatment temperatures [22–27]. Intermetallic compounds with mixed bonding (covalent bonds, metallic bonds and ionic bonds) play an important role in the mechanical behaviors and will significantly affect the electrical properties of laminated composites [28–30].

Different deformation characteristics of Ti and Cu plates during the rolling process are due to the difference in their physical properties. It is necessary to adopt preheating treatment or special rolling method to reduce the difference in plastic deformation resistance between the two metals to ensure high bonding strength at the interface [31,32]. The roll bonding techniques with corrugated rollers can be used to produce laminated composites of dissimilar metals, and uneven plastic deformation is obtained during the rolling process to improve a good interface. In previous work [33], corrugatedwith-flat rolling for one pass and flat-with-flat rolling for two passes were used to produce Mg/Al laminated composites, and the microstructural evolution and mechanical behavior of the laminated composites were investigated. A strong bonding is obtained at the Mg/Al interface, thereby achieving the excellent mechanical properties and good sheet shape of the Mg/Al laminated composites. The microstructure and mechanical behavior of Cu/Al laminated composites formed by the corrugatedwith-flat rolling process have been studied in detail [34]. It is observed that the fine grains near the interface and the high interface bonding strength of the Cu/Al laminated composites can be attributed to the inhomogeneous strain induced by the corrugated roller. However, the effect of longitudinal corrugated rolling on the microstructure and mechanical properties of Ti/Cu/Ti laminated composites has been less studied in detail, and its underlying mechanism is still unclear.

In this study, Ti/Cu/Ti laminated composites were prepared by a novel longitudinal corrugated rolling. The mechanical properties and micro-

structure of the laminated composites produced by longitudinal corrugated rolling were investigated, and compared with the traditional flat rolling method. The finite element method was used to analyze the strain field of Ti/Cu/Ti laminated composites.

2 Experimental

Industrially pure titanium TA1 and red copper T2 were adapt as raw materials. Along the rolling direction, the Ti and Cu plates were cut into the sizes of 100 mm × 20 mm × 0.3 mm and 100 mm × 20 mm × 2 mm, respectively. Ti and Cu plates were assembled in a "sandwich" form. Ti plates were located on both sides, Cu was located in the middle, and both ends of the slab were fixed with aluminum wire. Under vacuum condition, it was heated to 600 °C at a heating rate of 10 °C/min and kept for 5 min, and then rolled immediately.

The rolling process diagram of Ti/Cu/Ti laminated composites is shown in Fig. 1. The self-made two-high rolling mill with upper and lower corrugated rollers (CR) and the flat rolling (FR) mill were used (Figs. 1(a, b)). The rolling speed was maintained at 0.12 m/s and the reduction rate was 45%. The diameter of the corrugated and flat roll mill was 95 mm, and the surface curve of the corrugated roll was designed as sinusoidal curve with an amplitude of 0.35 mm and a period of 0.0698 rad/s.

The mechanical properties of the laminated composites along the rolling direction (RD) were evaluated by conducting 180° peel test and tensile test at room temperature through an electronic universal testing machine (Instron 5969). The peeling specimen with a length of 100 mm and a width of 5 mm was cut along the rolling direction of the laminated composites for a peel test. The crosshead speed was 5 mm/min. The tensile specimen with a gauge length of 20 mm and a gauge width of 5 mm was tested under uniaxial tension at a crosshead speed of 0.5 mm/min. The morphology and microstructure of each layer and interface layer of Ti/Cu/Ti laminated composites were observed by scanning electron microscope (SEM, Zeiss Gemini 300 and JMS-IT500) with energy spectrometer (EDS) and electron backscattering diffraction (EBSD).

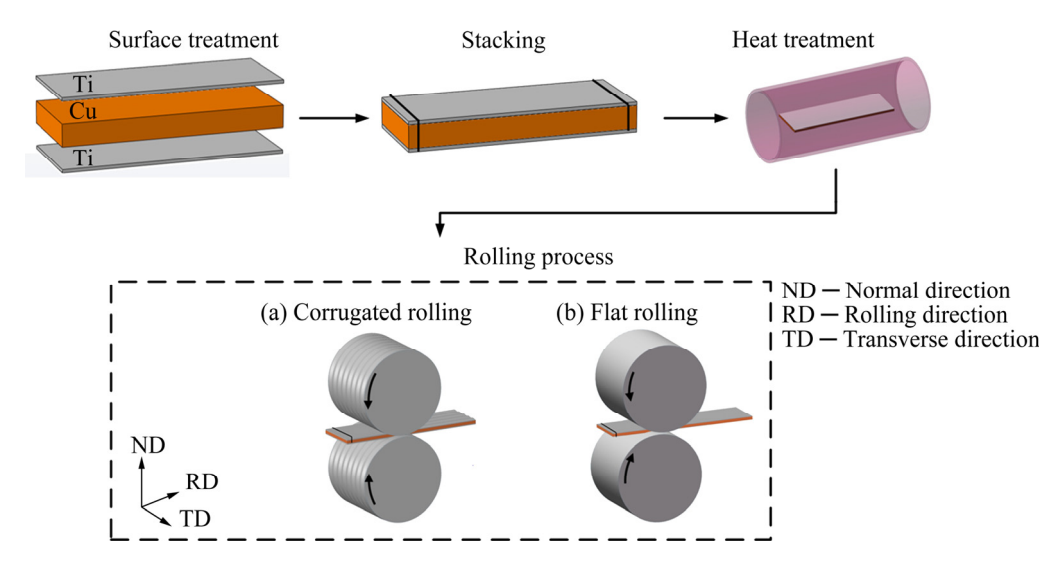


Fig. 1 Schematic diagram of rolling process of Ti/Cu/Ti laminated composites by CR and FR

The thermodynamic coupling process of Ti/Cu/Ti laminated composites produced by CR and FR was simulated using the ABAQUS finite element software. The rolls were both considered to be discrete rigid bodies, while Cu and Ti were defined as ideal elastic-plastic bodies, which were meshed by the type of C3D8R element. The material models of TA1 titanium and T2 copper were established by hot compression experiments performed on Gleeble-3800 thermomechanical simulator. The dimensions of the Ti and Cu plates were $100 \text{ mm} \times 20 \text{ mm} \times 0.3 \text{ mm}$ and $100 \text{ mm} \times$ 20 mm × 2 mm, respectively. The processing temperatures of Ti and Cu were both set to be 600 °C. The rolling speed was maintained at 0.12 m/s.

3 Results and discussion

3.1 Laminated morphologies of FR and CR composites

Figure 2 shows the SEM micrographs captured from section along the transverse direction of Ti/Cu/Ti laminated composites produced by FR and CR. It can be seen that no obvious delamination is observed at the interface of FR and CR laminated composites, indicating the good bonding between the Ti and Cu layers. The laminated composite rolled by FR is flat and straight as a whole. The laminated composite rolled by CR has a sinusoidally corrugated shape, which is consistent with the shape of the corrugated roll. The typical

positions at the interface of the CR laminated composite are marked as Trough I, Waist II and Peak III. Both the Ti and Cu layers deform uniformly in the transverse direction.

3.2 Interface microstructure characterization

Figure 3 shows the SEM micrographs of the interface regions of FR and CR laminated composites and its corresponding EDS spectra. Due to the different plastic deformation abilities of Ti and Cu, it can be seen from Figs. 3(a-d) that local cracks appear in the hard Ti layer, and the soft Cu layer tends to be stretched in the process of FR and CR. As a result, Cu is squeezed into the harder Ti. In addition, for the FR laminated composites, a "square" bonding interface is formed, and some defects, such as crack and hole, are observed in the rough interface area. For CR laminated composites, a "triangular" bonding interface is formed at the smooth interface positions of Trough I, Waist II and Peak III, and no visible defects (crack, hole, delamination, etc.) are observed in the interface area. The morphology of the bonding interface can affect the bonding strength of the interface in the deformation process of laminated composites [13]. EDS analysis shows evidence of atomic diffusion of Ti and Cu elements, and no oxide layers are observed in the interface area of FR and CR laminated composites. Note that there is a wider inter-diffusion zone in CR laminated composites. Compared with FR, the corrugated roll exacerbates the inhomogeneous strain and frictional

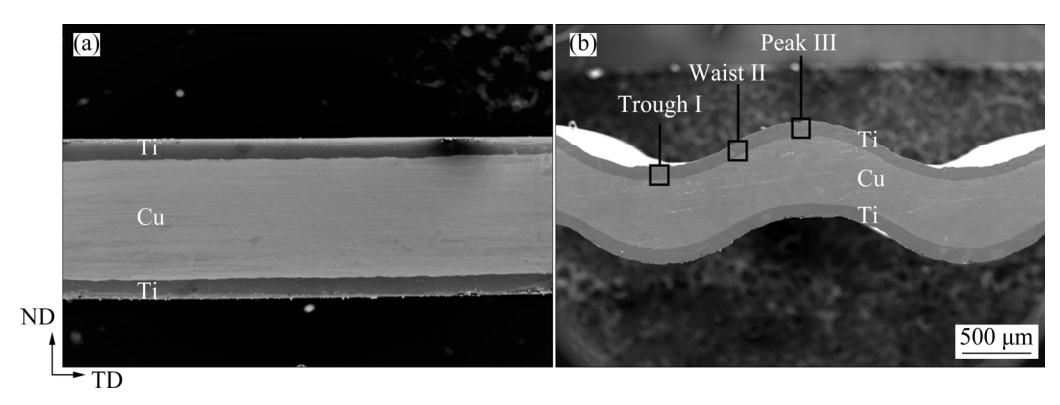


Fig. 2 SEM images of Ti/Cu/Ti laminated composites produced by FR (a) and CR (b)

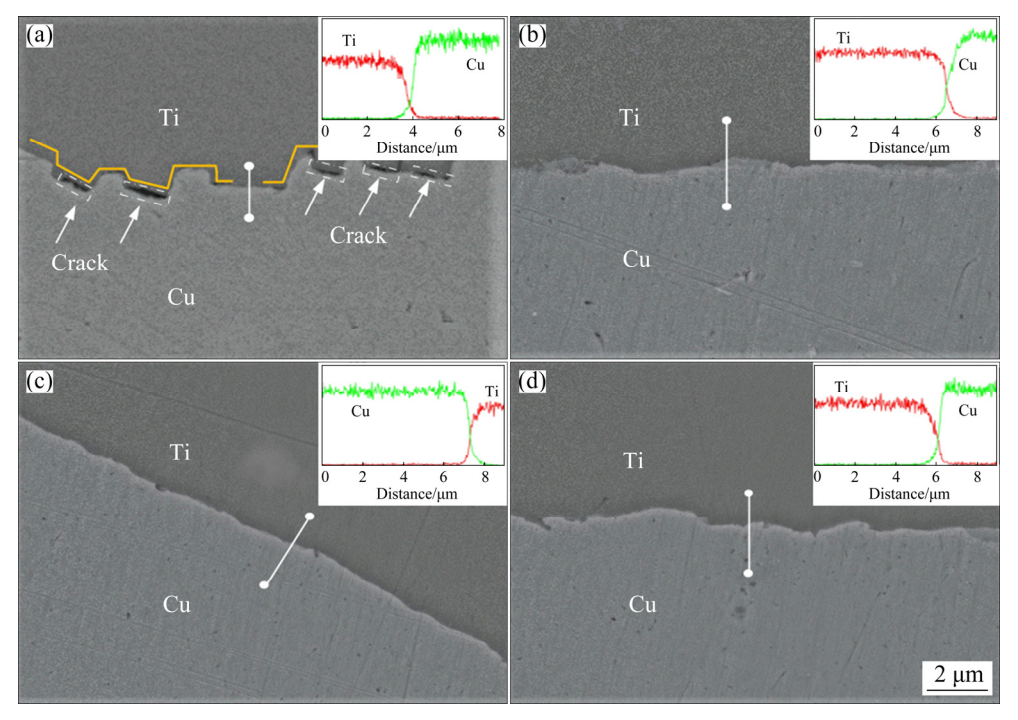


Fig. 3 SEM images and EDS line-scanning spectra of Ti/Cu interface regions for FR (a) and CR typical positions of Trough I (b), Waist II (c) and Peak III (d)

shear deformation of the laminated composites, facilitating the metal flow and atomic diffusion of Ti and Cu at the bonding interface [33,35]. The "triangular" bonding interface is formed under the action of heavy frictional shear deformation.

3.3 Interface bonding behavior

Figure 4 shows the peel test results of Ti/Cu/Ti laminated composites rolled by FR and CR. The average peel strengths are calculated according to Ref. [36]. The peel strength values of FR and CR laminated composites are 1.43 and 18.33 N/mm, respectively, indicating that the CR process has achieved a strong bonding in Ti/Cu/Ti laminated composites.

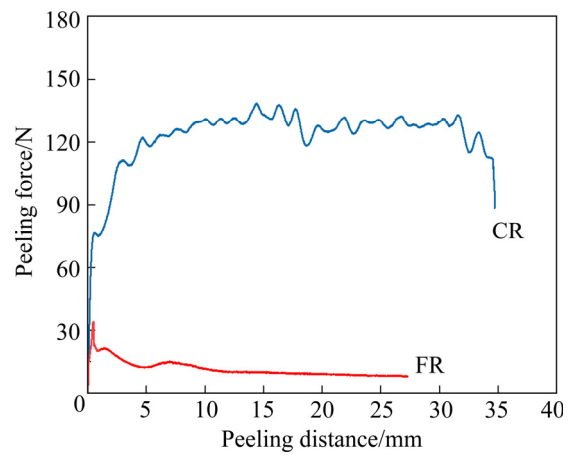


Fig. 4 Typical graphs of peeling force versus peeling distance for Ti/Cu/Ti laminated composites produced by FR and CR

Figure 5 shows the surface morphologies and element distributions of the peeled Ti layer. It can be found that discontinuous cracks are formed on the surface of the Ti layer, in which a small amount of residual Cu is attached, and the flat areas without copper show unbonded areas (Figs. 5(a, b)) [37]. It is inferred that non-uniform rupture of the Ti layer occurs during the FR process, and the metal Cu is squeezed into the cracks of the Ti layer in a local area, and the debonding phenomenon of Cu and Ti

appear during the peeling test. A large number of dimples appear in the Ti layer of CR at Trough I after peeling, while more Cu elements are distributed in the more obvious dimple regions (Figs. 5(c, d)). This suggests the strong bonding between Cu and Ti composites. At Waist II, a large amount of Cu is distributed in the cracks of the peeled Ti layer, forming a rough peeling surface with a few flat and debonding areas (Figs. 5(e, f)). This is related to the degree of plastic deformation

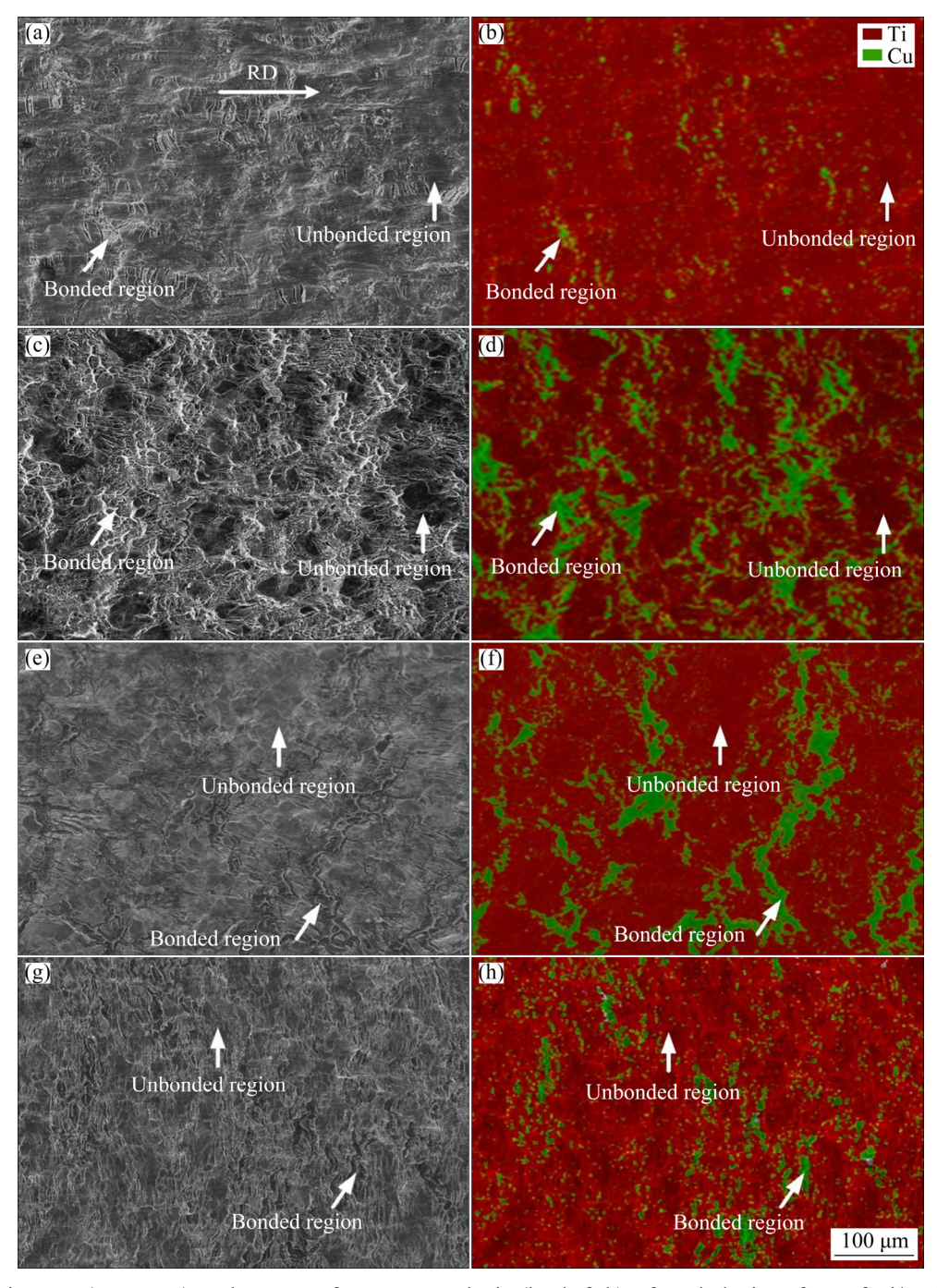


Fig. 5 SEM images (a, c, e, g) and EDS surface scan analysis (b, d, f, h) of peeled Ti surface of Ti/Cu/Ti laminated composites produced by FR (a, b) and CR typical positions of Trough I (c, d), Waist II (e, f) and Peak III (g, h)

of Ti and Cu layers at Waist II under the action of CR. The long crack zone of extruded Cu metal exists at CR Peak III, indicating the occurrence of cracks propagation due to the severe plastic deformation of the Ti and Cu layers during the CR process (Figs. 5(g, h)). This confirms that the CR process promotes the rupture of the passivated layer and the crack propagation on the surface of the Ti layer. This is beneficial to squeezing fresh Cu into the Ti layer and increasing the bonding strength between the Ti and Cu layers.

3.4 Tensile properties and fractography characteristics

Figure 6 exhibits engineering stress-strain curves of Ti/Cu/Ti laminated composites by FR and CR. It can be observed that CR composites possess higher tensile strength and ductility. The obvious change in ductility may be related to the grain refinement of the Ti and Cu layers due to the server plastic deformation during the CR process. On the other hand, this may be attributed to the good interface bonding of CR composites, and no debonding or separation in the interface areas is observed in the tensile test.

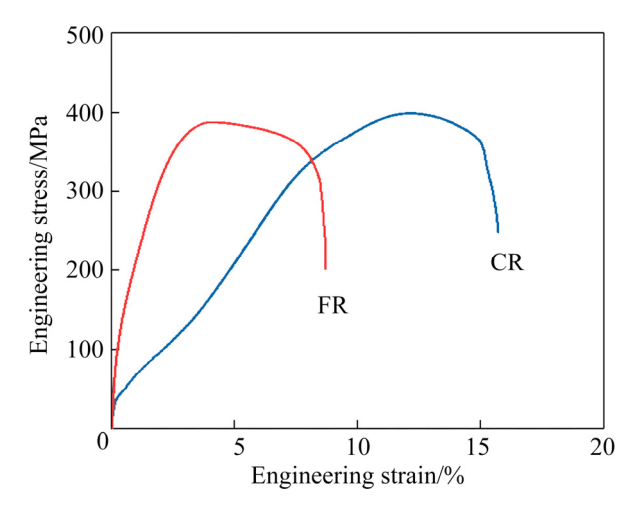


Fig. 6 Engineering stress-strain curves of Ti/Cu/Ti laminated composites by FR and CR

The SEM micrographs of the fracture surfaces of Ti/Cu/Ti laminated composites after tensile test is shown in Fig. 7. It is seen from Fig. 7(a) that the inclined fracture surface appears in the FR composites. According to the side-view fracture images (Figs. 7(c, e, g), debonding and separation are observed between the Ti and Cu layers, while a large number of dimples are distributed in the Ti

layer. It is demonstrated that there is interlaminar separation in the FR composite before the tensile fracture. After the Ti layer fractures, Cu rapidly fractures during the continued stretching process due to its low strength. From Figs. 7(b, d, f, h), it can be seen that the CR composites exhibit a flat and straight fracture surface, and there is no obvious debonding or separation of the interface layer. Meanwhile, dimples can be observed on the fracture surfaces of the Ti and Cu layers, which are similar to the dimples formed by ductile fracture [38]. It can be deduced that the Ti and Cu layers are plastically deformed together and then elongated until fracture during tensile test, indicating the strongest bonding interface formed in the ductile CR composites.

3.5 Deformation characteristics of FR and CR composites

Figure the equivalent strain shows distribution between the Ti and Cu layers of the Ti/Cu/Ti laminated composites formed by CR and FR. Corresponding to the rolling cycle of CR, the complete corrugation cycle of the finite element simulation is intercepted. It is seen that the effective plastic strains of the Ti and Cu layers of the CR laminated composites at Trough I and Waist II are higher than those of the FR sample, while the effective plastic strain at Peak III is lower than that of the FR sample. This shows that there are differences in the equivalent plastic strain at different positions in a complete wave cycle. The highest equivalent plastic strains of Ti and Cu layers appear at Trough I, and the lowest strains appear at Peak III. For CR and FR laminated composites, the effective plastic strain of the Ti layer is greater than that of the Cu layer, and especially under the action of CR, the Ti layer undergoes severe plastic deformation. Obviously, the larger normal stress and frictional shear stress play an important role in the deformation of the Ti layer in the CR process.

Figure 9 shows the EBSD orientation maps of the Ti and Cu layers at the interface of Ti/Cu/Ti laminated composites. For the FR laminated composites, the grains in the Cu layer are elongated along the rolling direction, and the grain size distribution ranges from 1 to 30 μ m, while the average grain size in the Ti layer is 2.3 μ m. At the

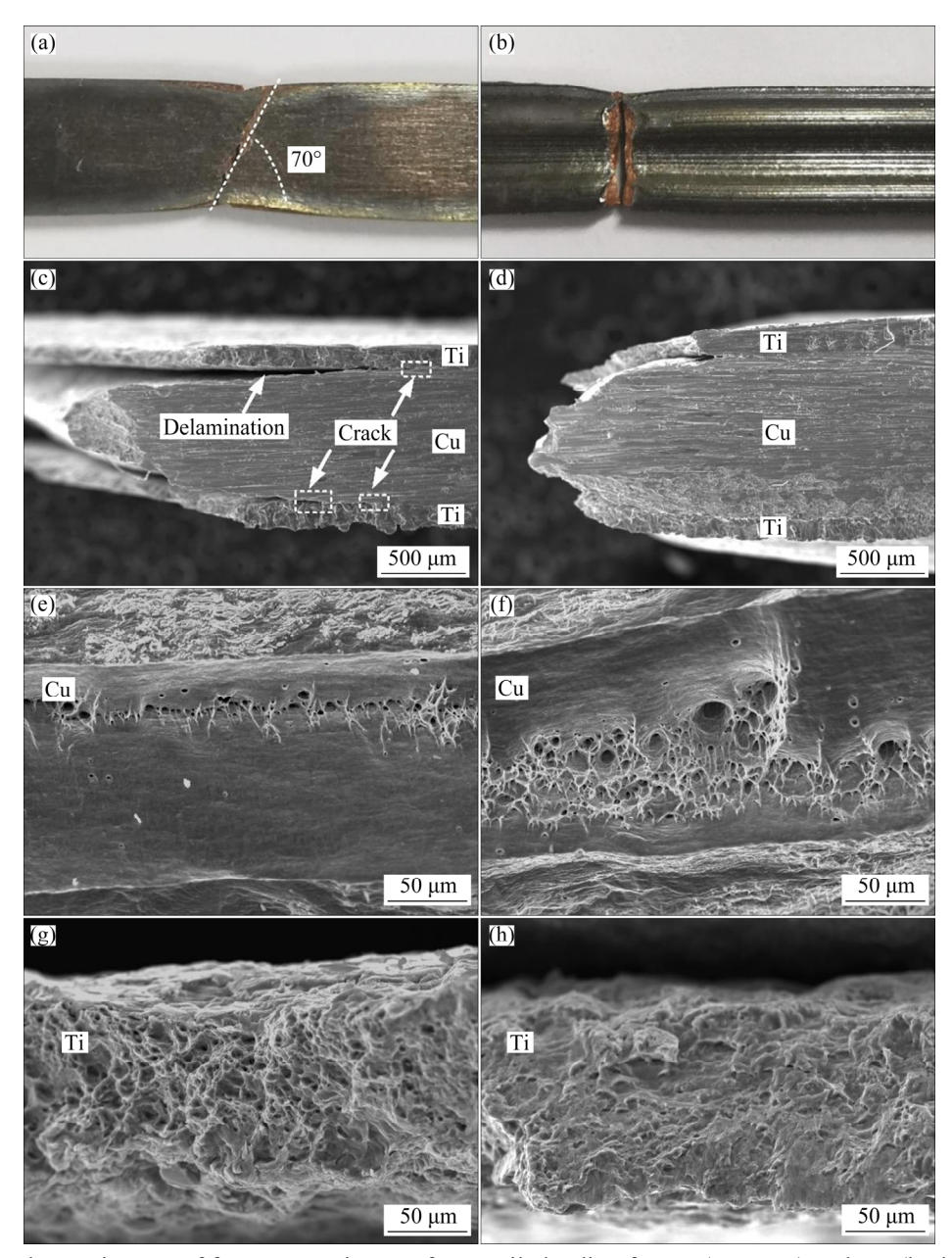


Fig. 7 Photos and SEM images of fracture specimens after tensile loading for FR (a, c, e, g) and CR (b, d, f, h)

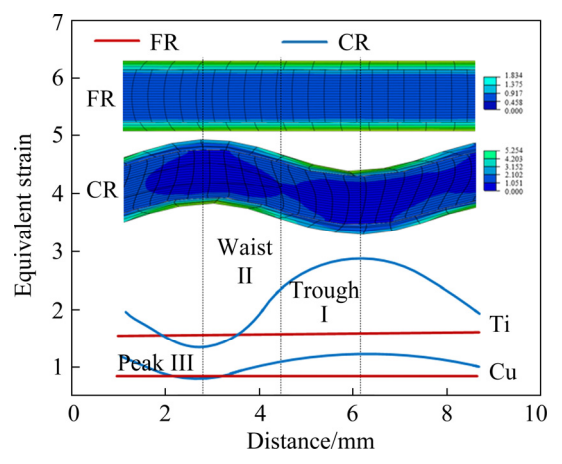


Fig. 8 Equivalent strain distribution in interface region of Ti/Cu/Ti laminated composites

positions of Trough I, Waist II and Peak III in the CR laminated composites, the average grain sizes of the Cu layer are 1.9, 1.3 and 3 µm, respectively, and the average grain sizes of the Ti layer are 2.1, 1.7 and 3.1 µm, respectively. Compared with FR composites, the grain refinement at Trough I and Waist II can be attributed to the grain breakage caused by severe plastic deformation under the action of CR. The grain size of Cu layer at Peak III decreases, which may be caused by dislocation entanglement and the increase of dislocation density at Trough I and Waist II, leading to the grain breakage. The grain growth at Trough I may be attributed to dynamic recrystallization [21].

3.6 Texture evolution

Figure 10 shows the ODF sections of the Ti and Cu layers at the interface of Ti/Cu/Ti laminated composites. The texture components at the interface of Ti and Cu layers by FR (Figs. 10(a, b)) are composed of near pyramidal texture of $\{02\overline{2}1\}\langle 2\overline{1}\overline{10}\rangle$ and near S $\{123\}\langle 634\rangle$ orientations, corresponding to the Euler space angles of $\{\varphi_1=0^\circ, \varphi=72^\circ, \varphi_2=30^\circ\}$ and $\{\varphi_1=60^\circ, \varphi=35^\circ, \varphi_2=65^\circ\}$,

respectively. These textures belong to the typical deformation textures in the Ti and Cu layers of FR composites [39–41]. Texture components at Trough I of CR Ti layer are $\{10\,\overline{1}3\}\langle11\overline{2}0\rangle$ located at the position of $\{\varphi_1=0^\circ,\ \varphi=32^\circ,\ \varphi_2=30^\circ\}$ (Fig. 10(c)), which belongs to a recrystallization texture [11], while the texture $\{1\,\overline{1}20\}\langle10\,\overline{1}0\rangle$ with the maximum intensity $\{\varphi_1=0^\circ,\ \varphi=90^\circ,\ \varphi_2=30^\circ\}$ exhibits at Waists II (Fig. 10(e)). It can be found

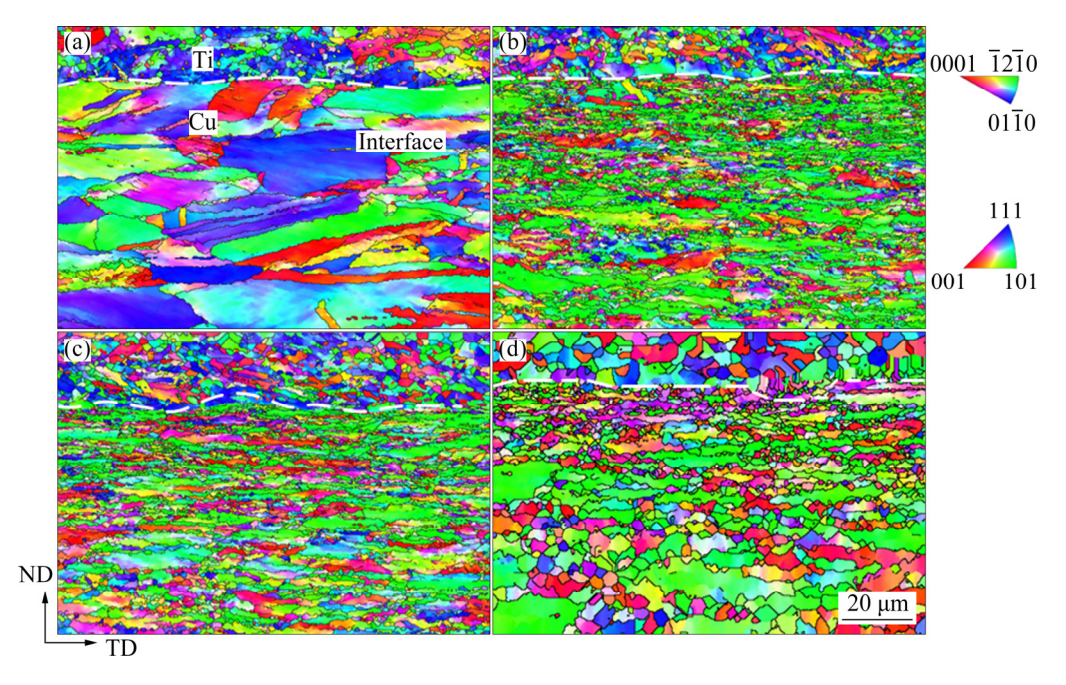


Fig. 9 EBSD orientation maps of Ti/Cu/Ti laminated composites produced by FR (a) and CR typical positions of Trough I (b), Waist II (c) and Peak III (d)

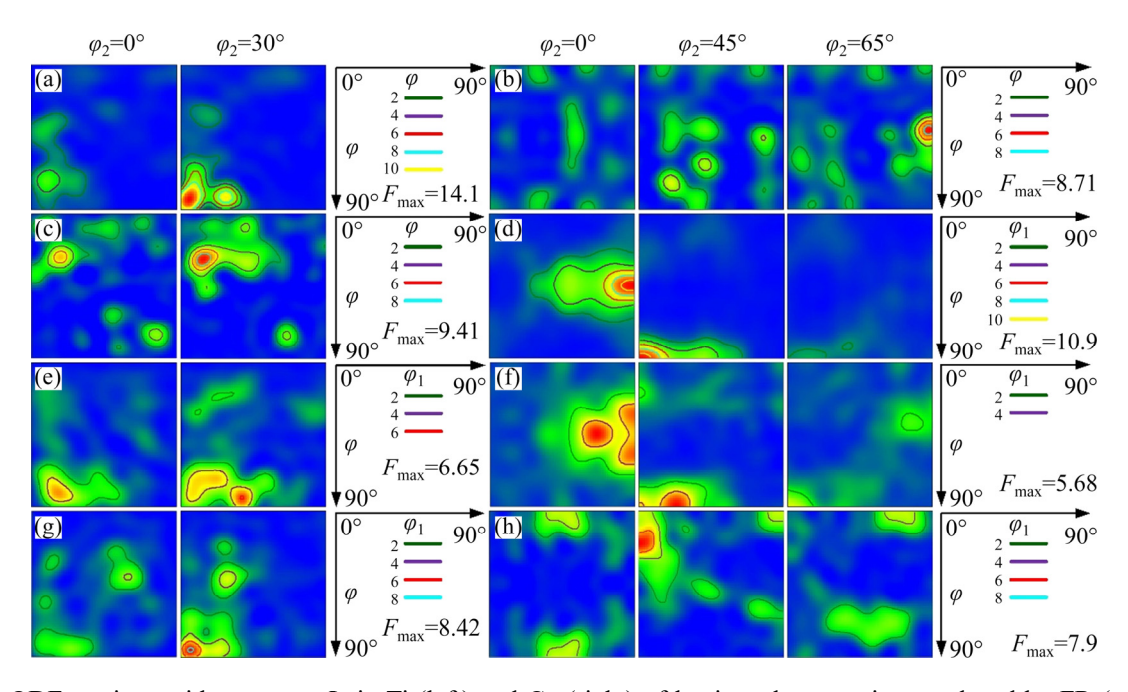


Fig. 10 ODF sections with constant Φ_2 in Ti (left) and Cu (right) of laminated composites produced by FR (a, b) and CR typical positions of Trough I (c, d), Waist II (e, f) and Peak III (g, h)

that the textures at Peak III are consistent with the FR Ti layer (Fig. 10(g)). This indicates that the recrystallization texture, prismatic and pyramidal texture are formed simultaneously as the equivalent strain of the Ti layer increases at the trough, waist and peak positions. The R-Goss $\{110\}\langle 110\rangle$ texture appears at the trough and waist positions of the CR Cu layer, indicating that dynamic recrystallization occurs at the trough and waist positions of the Cu layer. The near shear $\{001\}\langle 110\rangle$ texture at the waist is formed under the shear deformation because the Cu layer at Waist II is mainly subjected to the friction action [42]. The results show that when the force is transferred to the Cu layer, the normal stress and frictional shear force acting on the Cu layer are reduced, and the frictional shear stress may play a major role in the deformation of the Cu layer.

4 Conclusions

- (1) The CR laminated composite possesses a higher interfacial bonding strength due to the increased deformation of the Ti and Cu layers during the rolling process. A large number of crack areas in the Ti layer promote the combination of the Ti layer and the Cu layer.
- (2) The CR laminated composite has greater tensile strength and high ductility due to the grain refinement and strong interface bonding between the Ti and Cu layers.
- (3) The Ti and Cu layers of FR laminated composite exhibit typical deformation texture of $\{02\overline{2}1\}\langle 2\overline{1}\overline{1}0\rangle$ and $\{123\}\langle 634\rangle$. With the increase of plastic deformation at the trough, waist and peak positions of the CR laminated composite, the Ti layer exhibits recrystallization texture, prismatic and pyramidal texture, while the Cu layer exhibits R-Goss and shear orientation.

Acknowledgments

This study is financially supported by the National Key R&D Program of China (No. 2018YFA0707300), the Natural Science Foundation of Shanxi Province, China (No. 201801D221131), the National Natural Science Foundation of China (Nos. 51905372, 51904206, 51805359, 52075359), Shanxi Province Science and Technology Major Project, China (No. 20181102011), and China Postdoctoral Science Foundation (No. 2020M670705).

References

- [1] DEVILLIERS D, MAHE E. Modified titanium electrodes: Application to Ti/TiO₂/PbO₂ dimensionally stable anodes [J]. Electrochimica Acta, 2010, 55(27): 8207–8214.
- [2] ZHANG Wei, GHALI E, HOULACHI G. Review of oxide coated catalytic titanium anodes performance for metal electrowinning [J]. Hydrometallurgy, 2017, 169: 456–467.
- [3] GAO Mei-lian, WU Xiao-bo, GAO Ping-ping, LEI Ting, LIU Chun-xuan, XIE Zhi-yong. Properties of hydrophobic carbon-PTFE composite coating with high corrosion resistance by facile preparation on pure Ti [J]. Transactions of Nonferrous Metals Society of China, 2019, 29: 2321-2330.
- [4] BABAEI T, ZAREI M, HOSSEINI M G, HOSSEINI M M. Electrochemical advanced oxidation process of phenazopyridine drug waste using different Ti-based IrO₂—Ta₂O₅ anodes [J]. Journal of the Taiwan Institute of Chemical Engineers, 2020, 117: 103–111.
- [5] SONG Yan-fang, LIU Jia-man, GE Fang, HUANG Xin, ZHANG Yi, GE Hong-hua, MENG Xin-jing, ZHAO Yu-zeng. Influence of Nd-doping on the degradation performance of Ti/Sb-SnO₂ electrode [J]. Journal of Environmental Chemical Engineering, 2021, 9(4): 105409.
- [6] WANG Lin, DU Qing-lin, LI Chang, CUI Xiao-hui, ZHAO Xing, YU Hai-liang. Enhanced mechanical properties of lamellar Cu/Al composites processed via high-temperature accumulative roll bonding [J]. Transactions of Nonferrous Metals Society of China, 2019, 29: 1621–1630.
- [7] DEMIDENKO L Y, ONATSKAYA N A. Solid-state welding of tubular joints of titanium and copper with application of electrohydropulse loading [J]. Surface Engineering and Applied Electrochemistry, 2008, 44(3): 245–247.
- [8] MAO Yue, NI Yu, XIAO Xuan, QIN Ding-qiang, FU Li. Microstructural characterization and mechanical properties of micro friction stir welded dissimilar Al/Cu ultra-thin sheets [J]. Journal of Manufacturing Processes, 2020, 60: 356–365.
- [9] WEI Huan, HOU Li-feng, CUI Yan-chao, WEI Ying-hui. Effect of Ti content on corrosion behavior of Cu-Ti alloys in 3.5% NaCl solution [J]. Transactions of Nonferrous Metals Society of China, 2018, 28: 669-675.
- [10] FU Shao-li, CHEN Xiao-hong, LIU Ping. Preparation of CNTs/Cu composites with good electrical conductivity and excellent mechanical properties [J]. Materials Science & Engineering A, 2020, 771: 138656.
- [11] GUAN Qi-long, ZHANG Hui-jie, LIU Hui-jie, GAO Qiu-zhi, GONG Ming-long, QU Fu. Structure-property characteristics of Al-Cu joint formed by high-rotation-speed friction stir lap welding without tool penetration into lower Cu sheet [J]. Journal of Manufacturing Processes, 2020, 57: 363-369.
- [12] HE Yuan-huai, ZHOU Sheng-gang, ZHU Pei-xian, ZHANG Jin. Investigation on fabrication and properties of a novel Ti-Cu composited substrate electrode [J]. Journal of Kunming University of Science and Technology, 2015, 40(3):

- 27-31. (in Chinese)
- [13] HAN Z, ZHU P, ZHOU S, GUO Y Z, YANG Y. Study on preparation and properties of novel Ti/Cu laminated composite electrode materials [J]. Journal of New Materials for Electrochemical Systems, 2016, 19(2): 77–83.
- [14] AYDIN K, KAYA Y, KAHRAMAN N. Experimental study of diffusion welding/bonding of titanium to copper [J]. Materials and Design, 2012, 37: 356–368.
- [15] LEE J S, SON H T, OH I H, KANG C S, YUN C H, LIM S C, KWON H C. Fabrication and characterization of Ti–Cu clad materials by indirect extrusion [J]. Journal of Materials Processing Technology, 2007, 187: 653–656.
- [16] YANG Hong-mei, ZHU Pei-xian, ZHOU Sheng-gang, XU Jian, MA Hui-yu, GUO Jia-xin. Preliminary research on interfacial evolution behaviour of Ti-Cu laminated composite materials [J]. Advanced Engineering Materials, 2011, 194: 1615–1619.
- [17] KAHRAMAN N, GULENC B. Microstructural and mechanical properties of Cu–Ti plates bonded through explosive welding process [J]. Journal of Materials Processing Technology, 2005, 169: 67–71.
- [18] ZU Guo-yin, LI Xiao-bing, ZHANG Jing-hua, ZHANG Hao. Interfacial characterization and mechanical property of Ti/Cu clad sheet produced by explosive welding technology and annealing [J]. Journal of Wuhan University of Technology—Materials Science Edition, 2015, 30(6): 1198–1203.
- [19] HOSSEINI M, MANESH H D. Bond strength optimization of Ti/Cu/Ti clad composites produced by roll-bonding [J]. Materials & Design, 2015, 81: 122–132.
- [20] JIANG Shuang, PENG Ru-lin, JIA Nan, ZHAO Xiang, ZUO Liang. Microstructural and textural evolutions in multilayered Ti/Cu composites processed by accumulative roll bonding [J]. Journal of Materials Science & Technology, 2019, 35(6): 1165–1174.
- [21] KIM Y K, POURALIAKBAR H, HONG S I. Effect of interfacial intermetallic compounds evolution on the mechanical response and fracture of layered Ti/Cu/Ti clad materials [J]. Materials Science & Engineering A, 2020, 772: 138802.
- [22] YU Fei-fei, WANG He-feng, YUAN Guo-zheng, SHU Xue-feng. Effect of Cu content on wear resistance and mechanical behavior of Ti-Cu binary alloys [J]. Applied Physics A, 2017, 123(4): 278.
- [23] SHMORGUN V G, EVSTROPOV D A, TRUNOV M D. Investigation of the diffusion processes at the Interface of the Cu/Ti metal composite [J]. Materials Science Forum, 2016, 870: 239–242.
- [24] LAI A, BHANUMURTHY K, KALE G B, KASHYAP B P. Diffusion characteristics in the Cu–Ti system [J]. International Journal of Materials Research, 2012, 103(6): 661–672.
- [25] FAN Yong-gang, FAN Jun-xiang, WANG Cong. Formation of typical Cu–Ti intermetallic phases via a liquid–solid reaction approach [J]. Intermetallics, 2019, 113: 106577.
- [26] HAYAMA A O F, ANDRADE P N, CREMASCO A, CONTIERI R J, AFONSO C R M, CARAM R. Effects of composition and heat treatment on the mechanical behavior of Ti-Cu alloys [J]. Materials & Design, 2014, 55: 1006-1013.

- [27] CAMPO K N, LIMA D D D, LOPES E S N, CARAM R. On the selection of Ti-Cu alloys for thixoforming processes: Phase diagram and microstructural evaluation [J]. Journal of Materials Science, 2015, 50: 8007-8017.
- [28] YU Hai-liang, TIEU A K, LU Cheng, LIU Xiong, GODBOLE A, LI Hui-jun, KONG C, QIN Qing-hua. A deformation mechanism of hard metal surrounded by soft metal during roll forming [J]. Scientific Reports, 2014, 4: 5017.
- [29] JR K G, RUSSELL A, PECHARSKY A, MORRIS J, ZHANG Zhe-hua, LOGRASSO T, HSU D, LO C H C, YE Yi-ying, SLAGER A, KESSE D. A family of ductile intermetallic compounds [J]. Nature Materials, 2003, 2(9): 587–591.
- [30] PAUL H, SKUZA W, CHULIST R, MISZCZYK M, GALKA A, PRAZMOWSKI M, PSTRUS J. The effect of interface morphology on the electro-mechanical properties of Ti/Cu clad composites produced by explosive welding [J]. Metallurgical and Materials Transactions A, 2020, 51(2): 750–766.
- [31] HOSSEINI M, MANESH H D, EIZADJOU M. Development of high-strength, good-conductivity Cu/Ti bulk nano-layered composites by a combined roll-bonding process [J]. Journal of Alloys and Compounds, 2017, 701: 127–130.
- [32] HOSSEINI M, PARDIS N, MANESH H D, ABBASI M, KIM D I. Structural characteristics of Cu/Ti bimetal composite produced by accumulative roll-bonding (ARB) [J]. Materials & Design, 2017, 113: 128–136.
- [33] WANG Tao, WANG Yue-lin, BIAN Li-ping, HUANG Qing-xue. Microstructural evolution and mechanical behavior of Mg/Al laminated composite sheet by novel corrugated rolling and flat rolling [J]. Materials Science and Engineering A, 2019, 765: 138318.
- [34] LI Sha, LUO Chao, LIU Zhi-dong, ZHAO Jing-wei, HAN Jian-chao, WANG Tao. Interface characteristics and mechanical behavior of Cu/Al clad plate produced by the corrugated rolling technique [J]. Journal of Manufacturing Processes, 2020, 60: 75–85.
- [35] WANG Tao, LI Sha, REN Zhong-kai, HAN Jian-chao, HUANG Qing-xue. A novel approach for preparing Cu/Al laminated composite based on corrugated roll [J]. Materials Letters, 2019, 234: 79–82.
- [36] ABBASI M, TOROGHINEJAD M R. Effects of processing parameters on the bond strength of Cu/Cu roll-bonded strips [J]. Journal of Materials Processing Technology, 2010, 210(3): 560-563.
- [37] WANG Chun-yang, JIANG Yan-bin, XIE Jian-xin, ZHOU De-jing, ZHANG Xiao-jun. Interface formation and bonding mechanism of embedded aluminum—steel composite sheet during cold roll bonding [J]. Materials Science and Engineering A, 2017, 708: 50–59.
- [38] ELREFAEY A, TILLMANN W. Solid state diffusion bonding of titanium to steel using a copper base alloy as interlayer [J]. Journal of Materials Processing Technology, 2009, 209(5): 2746–2752.
- [39] LIU Jaan-ming, CHEN In-gann, CHOU Tung-sheng, CHOU Sheh-shon. On the deformation texture of square-shaped deep-drawing commercially pure Ti sheet [J]. Materials Chemistry and Physics, 2003, 77: 765–772.

- [40] YU Hai-ping, JIN Yan-ye, HU Lan, WANG Yu. Mechanical properties of the solution treated and quenched Al-Cu-Li alloy (AA2195) sheet during high strain rate deformation at room temperature [J]. Materials Science and Engineering A, 2020, 793: 139880.
- [41] FAN Cai-he, ZHENG Dong-sheng, CHEN Xi-hong, YANG Jian-jun, LIU Yong, LI Hui-zhong. Effect of large strain
- cross rolling on microstructure and properties of Al–Li alloy plates with high magnesium content [J]. Transactions of Nonferrous Metals Society of China, 2019, 29: 263–269.
- [42] WANG Miao, SHENG Jie, WANG Li-dong, YANG Zi-yue, SHI Zhen-dong, WANG Xiao-jun, FEI Wei-dong. Hot rolling behavior of graphene/Cu composites [J]. Journal of Alloys and Compounds, 2020, 816: 153204.

波纹辊和平辊轧制 Ti/Cu/Ti 层压复合材料的显微组织与力学性能

刘竹波 1,2,3, 王昕玥 1, 刘名硕 1, 刘元铭 1,2,3, 刘江林 1,2,3, A. V. IGNATOV4, 王 涛 1,2,3

- 1. 太原理工大学 机械与运载工程学院,太原 030024;
- 2. 太原理工大学 先进金属复合材料成形技术与装备教育部工程研究中心,太原 030024;
 - 3. 太原理工大学 中澳联合研究中心,太原 030024;
- 4. Department of Mechanical Engineering, Bauman Moscow State Technical University, Moscow 105005, Russia
- 摘 要:采用波纹辊和平辊轧制方法制备钛/铜/钛(Ti/Cu/Ti)层压复合板材料。通过扫描电镜、数值模拟、剥离和拉伸实验等方法研究层压复合板的显微组织和力学性能,对比分析波纹辊和平辊轧制效果。结果表明:波纹辊和平辊轧制的层压复合板在 Ti 层和 Cu 层界面处表现出不同的有效塑性应变分布。波纹辊轧制的层压复合板中,Ti 层具有再结晶织构、棱柱面织构和棱锥面织构,Cu 层形成高斯织构和剪切织构;而平辊轧制的层压复合板中,Ti 层和 Cu 层均具有典型的变形织构。波纹辊轧制的层压复合板材料具有较高的结合强度、抗拉强度和延展性。关键词:Ti/Cu/Ti 层压复合材料;波纹辊轧制;平辊轧制;结合强度;界面微观结构;有限元分析

(Edited by Bing YANG)